Cerebral Cortex, May 2017;27:2926–2940

doi:10.1093/cercor/bhw142
Advance Access Publication Date: 25 May 2016

ORIGINAL ARTICLE

Dual Cortical Plasticity After Spinal Cord Injury

Desire Humanes-Valera[1,2,†], Guglielmo Foffani[1,3,†], Elena Alonso-Calviño[1], Elena Fernández-López[1] and Juan Aguilar[1,†]

[1]Hospital Nacional de Parapléjicos, Servicio de Salud de Castilla-La Mancha, 45071 Toledo, Spain, [2]Department of Systems Neuroscience, Institute of Physiology, Faculty of Medicine, Ruhr-University Bochum, D-44801 Bochum, Germany and [3]CINAC, HM Puerta del Sur, Hospitales de Madrid, Móstoles, and CEU-San Pablo University, Madrid, Spain

Address correspondence to guglielmo.foffani@gmail.com (G.F); jdaguilar@sescam.jccm.es (J.A.)

[†]Desire Humanes-Valera, Guglielmo Foffani, and Juan Aguilar contributed equally to this work.

Abstract

During cortical development, plasticity reflects the dynamic equilibrium between increasing and decreasing functional connectivity subserved by synaptic sprouting and pruning. After adult cortical deafferentation, plasticity seems to be dominated by increased functional connectivity, leading to the classical expansive reorganization from the intact to the deafferented cortex. In contrast, here we show a striking "*decrease*" in the fast cortical responses to high-intensity forepaw stimulation 1–3 months after complete thoracic spinal cord transection, as evident in both local field potentials and intracellular in vivo recordings. Importantly, this decrease in fast cortical responses co-exists with an "*increase*" in cortical activation over slower post-stimulus timescales, as measured by an increased forepaw-to-hindpaw propagation of stimulus-triggered cortical up-states, as well as by the enhanced slow sustained depolarization evoked by high-frequency forepaw stimuli in the deafferented hindpaw cortex. This coincidence of diminished fast cortical responses and enhanced slow cortical activation offers a dual perspective of adult cortical plasticity after spinal cord injury.

Key words: cortical reorganization, neural plasticity, neurophysiology, somatosensory system, spinal cord injury

Introduction

Plasticity in the central nervous system (CNS) reaches a peak during development and it declines dramatically in adulthood (Wiesel and Hubel 1963; Huttenlocher 1979; Grutzendler et al. 2002; Holtmaat et al. 2005). Some processes of developmental plasticity can be reactivated in the adult brain (Pizzorusso et al. 2002; Maya Vetencourt et al. 2008), particularly after CNS lesion (Murphy and Corbett 2009; Yamahachi et al. 2009), and indeed, there is extensive literature regarding cortical plasticity after deafferentation that documents the classical functional enlargement of adjacent intact areas into deafferented areas (Wall and Egger 1971; Hubel et al. 1977; Calford and Tweedale 1988; Sanes et al. 1988; Kaas et al. 1990; Pons et al. 1991; Gilbert and Wiesel 1992; Das and Gilbert 1995; Schmid et al. 1996; Jain et al. 1997; Florence et al. 1998; Buonomano and Merzenich 1998; Harrison et al. 2013; Albieri et al. 2015). This expansive reorganization is associated with a wide scale remodeling of synapses and circuits, due to complex and coordinated synaptogenesis, axonal sprouting, and unmasking at cortical and subcortical levels (Jacobs and Donoghue 1991; Darian-Smith and Gilbert 1994; Fouad et al. 2001; Levy et al. 2002; Yamahachi et al. 2009; Vessal ad Darian-Smith 2010; Kambi et al. 2014).

However, classical expansive reorganization cannot fully explain the complex phenomenon of adult cortical reorganization after deafferentation (Giannikopoulos and Eysel 2006; Moxon et al. 2014). Developmental plasticity teaches us that sprouting coexists with pruning in a synergic and dynamic manner (Huttenlocher 1979; Mataga et al. 2004; Paolicelli et al. 2011), and it is now becoming progressively clear that axonal/synaptic pruning also plays a critical role in adult cortical plasticity after

deafferentation (Yamahachi et al. 2009; Keck et al. 2011; van Versendaal et al. 2012; Gilbert and Li 2012). Unfortunately, the functional implications of synaptic pruning in the deafferented adult brain remain elusive.

Spinal cord injury (SCI) in rodents is an appealing model in which the functional consequences of adult cortical deafferentation can be investigated, both because of its clinical relevance (Moxon et al. 2014) and due to the exquisite layer-specific synaptic pruning that occurs in the deafferented cortex (Kim et al. 2006; Ghosh et al. 2012; Zhang et al. 2015). In the somatosensory cortex, SCI seems to provoke classical long-term expansive reorganization, at least when studied by functional magnetic resonance imaging (fMRI) (Endo et al. 2007; Ghosh et al. 2010). Paradoxically though, no long-term cortical reorganization whatsoever can be detected through electrophysiological single-unit recordings (Jain et al. 1995; Graziano et al. 2013), unless rats are subjected to specific drug treatment and/or exercise regimes (Graziano et al. 2013; Ganzer et al. 2013; Foffani et al. 2016).

To reconcile these findings, the present study set out to establish an integrative electrophysiological framework of long-term reorganization of the somatosensory cortex after SCI. We adopted a 2-tier experimental strategy: first, to bridge the gap between the fast cellular level of single-unit recordings (Jain et al. 1995; Graziano et al. 2013; Foffani et al. 2016) and the slow metabolic level of fMRI (Endo et al. 2007; Ghosh et al. 2010), we investigated cortical reorganization at a population level through local field potentials (LFPs); second, to integrate the population results with responses at the cellular level, we performed in vivo intracellular recordings. We hypothesized that 2 modalities of cortical plasticity exist, with a possible dissociation between the reorganization of cortical responses over fast post-stimulus timescales and cortical activation over slower post-stimulus timescales.

Materials and Methods

Experiments were performed on male Wistar rats in accordance with the International Council for Laboratory Animal Science guidelines and the European Union regulation 2010/63/EU. All the experimental protocols were approved by the Ethical Committee for Animal Research at the Hospital Nacional de Parapléjicos (Toledo, Spain). Extracellular recordings were performed in 11 intact animals, 10 animals 1 week after SCI, 13 animals 1 month after SCI and 8 animals 3 months after SCI (Fig. 1). Intracellular recordings were obtained from 8 intact animals and immediately after SCI, and in 4 animals 1–3 months after SCI. Intact animals were housed 2 per cage in standardized cages, with food and water ad libitum, and kept at 23°C on a 12 h light/dark cycle. After spinal cord transection, all animals were housed individually in a nonenhanced environment and were handled for manual voiding of the bladder. No additional exercise was performed. The general experimental approach (anesthesia, surgery, extracellular recordings, and peripheral stimulation) is similar to that used in our previous studies (Aguilar et al. 2010; Yague et al. 2011, 2014; Humanes-Valera et al. 2013, 2014).

Surgery for Chronic SCI and Post-operative Care

Animals were anesthetized with Dolethal (50 mg/kg i.p.), and administered 2% Xylagesic (10 mg/kg) as a muscle relaxant and analgesic. The body temperature of the animals was kept constant (36.5°C) using an automatically controlled heating pad and their eyes were protected with ophthalmic gel. After anesthetizing the rats, the skin of the surgical area was shaved, swabbed with ethanol 70% and disinfected with Povidona iodine strips. A laminectomy was performed at thoracic level T9–T10, keeping both the musculature and vascularization in the surgical area intact. The dura mater was removed and the spinal cord was then completely transected, as confirmed visually under the surgical microscope by the total separation of the borders. After inflicting the SCI, the incision was carefully sutured and the animals were administered 2.5% Baytril and Buprex. The first day after the surgery the animal's bladder was emptied and they were administered 2.5% Baytril, 2.5% Buprex, and saline. Saline and Baytril continued to be administered for 1 week and the animal's bladder was emptied for 3 weeks after SCI.

Surgery for in vivo Anesthetized Electrophysiological Recordings

Animals were anesthetized with urethane (1.5 g/kg i.p.) and their body temperature was kept constant (36.5°C) using an automatically controlled heating pad. The animals were placed in a stereotaxic frame (SR-6 Narishige Scientific Instruments, Tokio, Japan) with their skull exposed and a craniotomy was performed on the right side of the midline over the primary somatosensory cortex: antero-posterior 1 to –4; medio-lateral 1–5 (Paxinos and Watson 2007). The cisterna magna was opened to decrease brain pressure and improve the stability of the recordings, as follows: an incision was made in the skin of the dorsal part of the neck; the posterior cranial muscles of the occipital bone were gently removed and separated 1–2 cm from the head, leaving the first 2 segments of cervical spinal cord and the posterior part of cerebellum over the obex visible and the dura exposed; a small incision on the dura was performed close to the occipital bone (where the dura is spatially separated from the caudal part of the medulla oblongata), causing a small quantity of cerebrospinal fluid to come out, which was visually confirmed under the microscope. This procedure releases most of the intracranial pressure that is responsible for brain movements due to the heart pulse and the breathing, allowing for more stable and long-lasting recordings. At cranial level, small incisions in the dura mater were made to allow the recording electrodes to be lowered into the cerebral cortex. Once the electrodes were located at the hindpaw and forepaw representations of the primary somatosensory cortex, we applied a few very-high intensity (10 mA) electrical stimulation pulses to the hindpaw to confirm that no physiological responses were evoked in the cortex by stimuli delivered below the level of the lesion. After confirming that the animal had complete SCI, we performed electrophysiological recordings under lighter anesthesia (stage III-3: Friedberg et al. 1999; Erchova et al. 2002). Additional doses of urethane (<one-sixth of the induction dose) were then administered in order to obtain a consistent state of deep slow-wave activity. In this state we performed the electrophysiological recordings under deeper anesthesia (stage III-4: Friedberg et al. 1999; Erchova et al. 2002).

Extracellular Electrophysiological Recordings

Extracellular recordings were obtained using tungsten electrodes with a 4–5 MΩ impedance at 1000 Hz (TM31C40KT and TM31A50KT: WPI Inc Sarasota, FL, USA). Two electrodes were stereotaxically lowered into the infragranular somatosensory cortex according to the coordinates of Chapin and Lin 1984), one in the forepaw area (antero-posterior 0.5 mm; medio-lateral 4 mm; depth 1.1–1.6 mm) and the other in the hindpaw area (antero-posterior –1 mm; medio-lateral 2.5 mm; depth 1.1–1.6 mm). Once fixed in place, the electrodes were not moved throughout the experiment. Ground and reference were placed in the parietal muscular tissue on opposite sides. All recordings

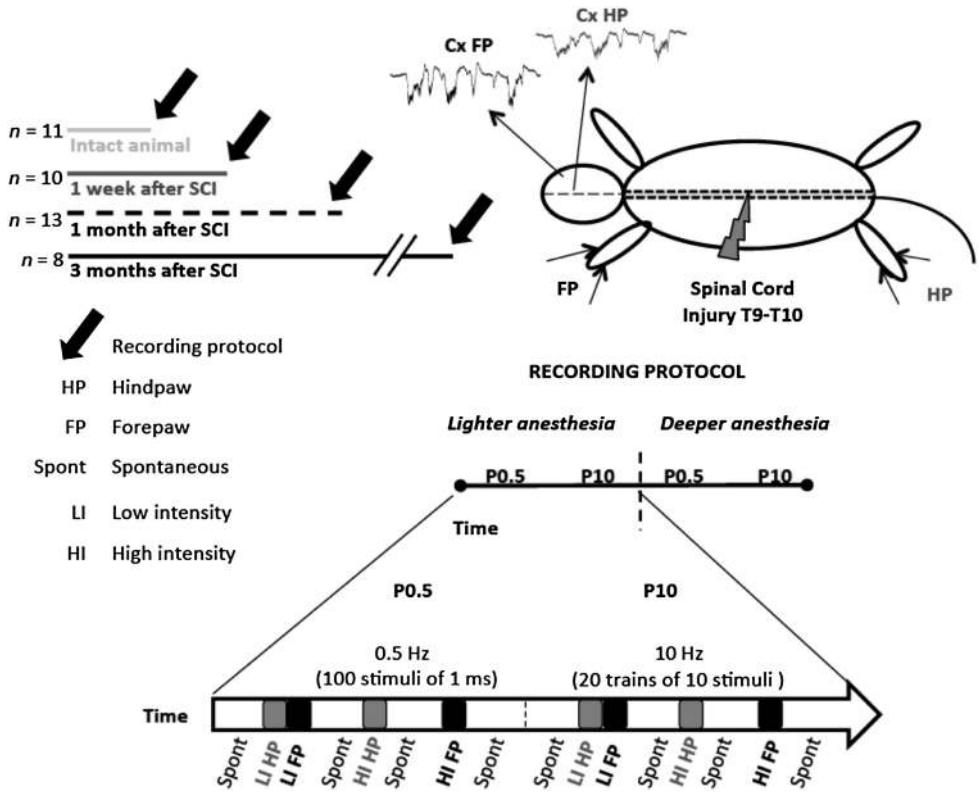

Figure 1. Experimental protocol. Extracellular recordings were obtained from the forepaw (FP) and hindpaw (HP) representations of the primary somatosensory cortex (Cx) in urethane-anaesthetized rats. The experiment was performed on different groups of animals: intact animals; 1 week, 1 month, and 3 months after SCI. Complete transection of the spinal cord was performed at the thoracic T9–T10 level, and we studied both the spontaneous activity and the responses evoked by electrical stimuli delivered to the forepaw at low (0.5 mA) and high intensity (5 mA). We used 2 stimulation frequencies: 0.5 Hz and 10 Hz. The first recording protocol was performed under lighter anesthesia and we then administered an additional dose of urethane to obtain a consistent state of slow-wave activity. In this state of deeper anesthesia we obtained the second recordings. The thick black arrow indicates when the recordings were obtained.

were pre-amplified in DC mode, low-pass filtered (<3 kHz) and amplified using a modular system (Neurolog, Digitimer Ltd.). Analog signals were converted into digital data at a 20 kHz sampling rate and with 16-bit quantization using a CED power 1401 (Cambridge Electronics Design, Cambridge, UK) controlled by Spike2 software (v6, Cambridge Electronics Design, Cambridge, UK). Signals were stored on the hard disk of a PC for later analysis.

Intracellular Electrophysiological Recordings

Intracellular recordings were obtained with sharp electrodes using an intracellular amplifier (Axoclamp 2B, Molecular Devices). Sharp electrodes were made from capillary tubes with intraluminal glass fibers (borosilicate, o.d. 1.5 mm, i.d. 0.86 mm; Harvard Apparatus), pulled on a Brown–Flaming horizontal puller (Model P-97; Sutter Instrument Co.) and filled with 2.5 M potassium acetate (electrode resistances: 40–80 MΩ). These recordings were included only if the resting membrane potentials during down-states were stable at values more negative than −60 mV, the action potentials were larger than 50 mV and the recording lasted longer than 10 min (range 10 min to 2 h). Intracellular data were acquired simultaneously and continuously at 20 kHz (CED1401 Cambridge Electronic Design, Cambridge, UK), with one extracellular channel in the forepaw cortex. The cisterna magna was opened and the cerebrospinal fluid was drained to decrease the pulsation of the brain and the cortex was covered with agar 4% to favor stability. All neurons were recorded in layer V (deep 1100–1700 μm). To electrophysiologically identify the neurons, we applied intracellular current pulses of 0.5–0.8 s duration during down-states, with increasing positive currents (+0.2; +0.4; +0.6; +0.8; +1 nA) and decreasing negative currents (−0.2; −0.4; −0.6; −0.8; −1 nA). Neurons that showed adaptation between the first few spikes and the last spikes of the pulse (in terms of increased inter-spike intervals) were classified as regular spiking (RS) or putative pyramidal cells, and neurons that showed no adaptation between the start and the end of the pulse were classified as fast spiking (FS) or putative interneurons (Contreras, 2004). In general, a linear relation was found between the pulse amplitude and the firing rate for both types of neuron, with a steeper slope for interneurons. We confirmed that the duration of the spike at half-amplitude was >0.8 ms for all pyramidal neurons recorded.

Peripheral Stimulation

Electrical pulses were applied using bipolar needle electrodes located subcutaneously at the wrist of the forepaw and hindpaw, one pole on each side of the paw. The rationale for this stimulation was to activate all types of somatosensory fibers originating within the paws, including tactile, proprioceptive, and nociceptive fibers. Two stimulation protocols were applied: 0.5 Hz (100 pulse stimuli with 1 ms duration) and 10 Hz (20 trains of 10 stimuli of 1 ms duration). Each stimulation protocol was delivered at 2 stimulus intensities: low-intensity (0.5 mA) and high-intensity (5 mA).

Data Analysis

Evoked Responses

LFPs were obtained by averaging the raw signals recorded from the electrodes across stimuli. The amplitude of the LFP responses was evaluated as the absolute value of the negative peak in the average response.

Spontaneous Activity

Spontaneous activity was studied in recordings of at least 150 s obtained immediately after the low-intensity stimulation and immediately before the high-intensity stimulation. To evaluate the level of cortical spontaneous activity quantitatively, we extracted the rectified multiunit activity (rMUA) by band-pass filtering the raw signals at high frequencies (300–3000 Hz) and rectifying the resulting signal.

Single-trial Analyses

Single-trial analyses were performed by quantifying the average rectified rMUA in the 45 ms before each stimulus and the peak-to-peak amplitude of the LFP response to the subsequent stimulus.

Intracellular data

The resting membrane potential (V_m) was measured during periods of down-states. We verified that the V_m was stable during down-states over the entire recording protocol, including responses to peripheral stimulation and spontaneous activity. Input resistance (R_m) was evaluated from the slope of the *I*/*V* plot using the intracellular current pulses. Synaptic responses to somatosensory stimuli were measured by averaging all the responses occurring during the down-states, after applying a median filter of 1.5 ms to eliminate the spikes. The amplitude of synaptic responses was measured as the peak depolarization within 50 ms post-stimulus. The slope of synaptic responses was measured by fitting a straight line between 5% and 95% of the peak response.

Adaptation

Paired-pulse adaptation was measured from the ratio between the average LFP response amplitude to the second and first stimulus of the 10 Hz train (second/first). Steady-state adaptation was measured as the ratio between the average LFP response amplitude to the tenth and first stimulus of the train (tenth/first).

Stimulus-triggered Up-States

Stimulus-triggered up-states were quantified both in the forepaw and hindpaw cortex from the LFP/MUA extracellular recordings. A stimulus was considered to have triggered an up-state if it satisfied the following criteria: (1) the stimulus occurred in a down-state (i.e., no cortical activity was observed in the 300 ms before the stimulus); (2) after the initial short-latency response, a long-latency activation (corresponding to an up-state) was observed within 200 ms of the stimulus. Stimulus-triggered up-states were then quantified in terms of probability, as the ratio of the number of stimuli that triggered an up-state and the number of stimuli that occurred in a down-state. As a control analysis, spontaneously triggered up states were automatically quantified from the MUA in 3 time periods: [t1] −200 to 0 ms before each stimulus; [t2] 500–700 ms after each stimulus; and [t3] 1000–1200 ms after each stimulus.

Slow Sustained Depolarization

Slow sustained depolarizations produced by high intensity 10 Hz stimuli were quantified as the absolute difference between the V_m during the pre-stimulus down-state and the average V_m during the 10 Hz train (1 s) or after the 10 Hz train (1 s).

Statistical Analyses

Statistical analyses were performed using 1-way, 2-way, or 3-way analyses of variance (ANOVA), with follow-up ANOVAs when appropriate and a Tukey Honest Significant Difference Test for post hoc comparisons. A squared-root transformation was used when necessary to guarantee normality and homoscedasticity. Correlations were assessed with Pearson correlation coefficient. All results were considered significant at $P < 0.05$.

Results

A Long-term Decrease in Fast Cortical Responses to Forepaw Stimuli After Thoracic Spinal Cord Transection

We obtained recordings from the hindpaw–forepaw somatosensory cortex of anesthetized rats, either under control conditions (intact animals) or 1 week, 1 month, or 3 months after complete thoracic (T9–T10) spinal cord transection (TX; Fig. 1). We first set out to obtain electrophysiological evidence of long-term cortical reorganization of fast cortical responses at the population level by recording LFPs from the infragranular hindpaw–forepaw somatosensory cortex. LFPs were chosen for their sensitivity to synaptic activity, thereby providing a suitable population measure to evaluate fast cortical responsiveness (Nemoto et al. 2004; Katzner et al. 2009; Aguilar et al. 2010), as well as their sensitivity to cortical adaptation (Castro-Alamancos 2004a) and plasticity (Megevand et al. 2009). The infragranular cortex was targeted because it plays a critical role in cortical input–output integration under physiological conditions (Murayama et al. 2009; Zarrinpar and Callaway 2016), it is sensitive to changes in excitability after deafferentation (Breton and Stuart 2009) and it is where most synaptic pruning occurs after SCI (Ghosh et al. 2012). We delivered both low (0.5 mA) and high intensity (5 mA) electrical stimuli to the contralateral forepaw, under the rationale that low-intensity stimuli specifically activate dorsal column pathways similar to more natural light mechanical stimuli (Lilja et al. 2006), while high-intensity stimuli activate all somatosensory pathways, ensuring the full engagement of cortical circuits involved in somatosensory processing (Lilja et al. 2006; Yague et al. 2011; Morales-Botello et al. 2012). To gain insight into the possible state dependence of cortical responsiveness after spinal cord transection (Aguilar et al. 2010), we recorded the LFP responses under 2 states of anesthesia (Humanes-Valera et al. 2013): lighter anesthesia (stage III-3) and deeper anesthesia (stage III-4; Friedberg et al. 1999; Erchova et al. 2002). Recordings were obtained simultaneously in the hindpaw cortex and in the forepaw cortex, which are maximally activated by stimuli below and above the level of the lesion, respectively.

In our experiments, complete thoracic spinal cord transection produced long-term effects in the fast LFP responses evoked in the infragranular hindpaw–forepaw cortex by a contralateral forepaw stimulus (3-way independent-measures ANOVA, TIME $F(3,229) = 10.6$, $P < 0.0001$: Figure 2A–C). Importantly, we did not observe classic long-term expansive cortical reorganization. While cortical responses were not significantly different in animals recorded 1 week after TX to those in intact animals (Tukey: $P = 0.61$), they were dramatically "*smaller*" in animals recorded 1 ($P < 0.0001$) and 3 months after TX ($P = 0.0006$). We studied this further by analyzing the responses evoked by high-intensity forepaw stimuli (5 mA) in the deafferented hindpaw

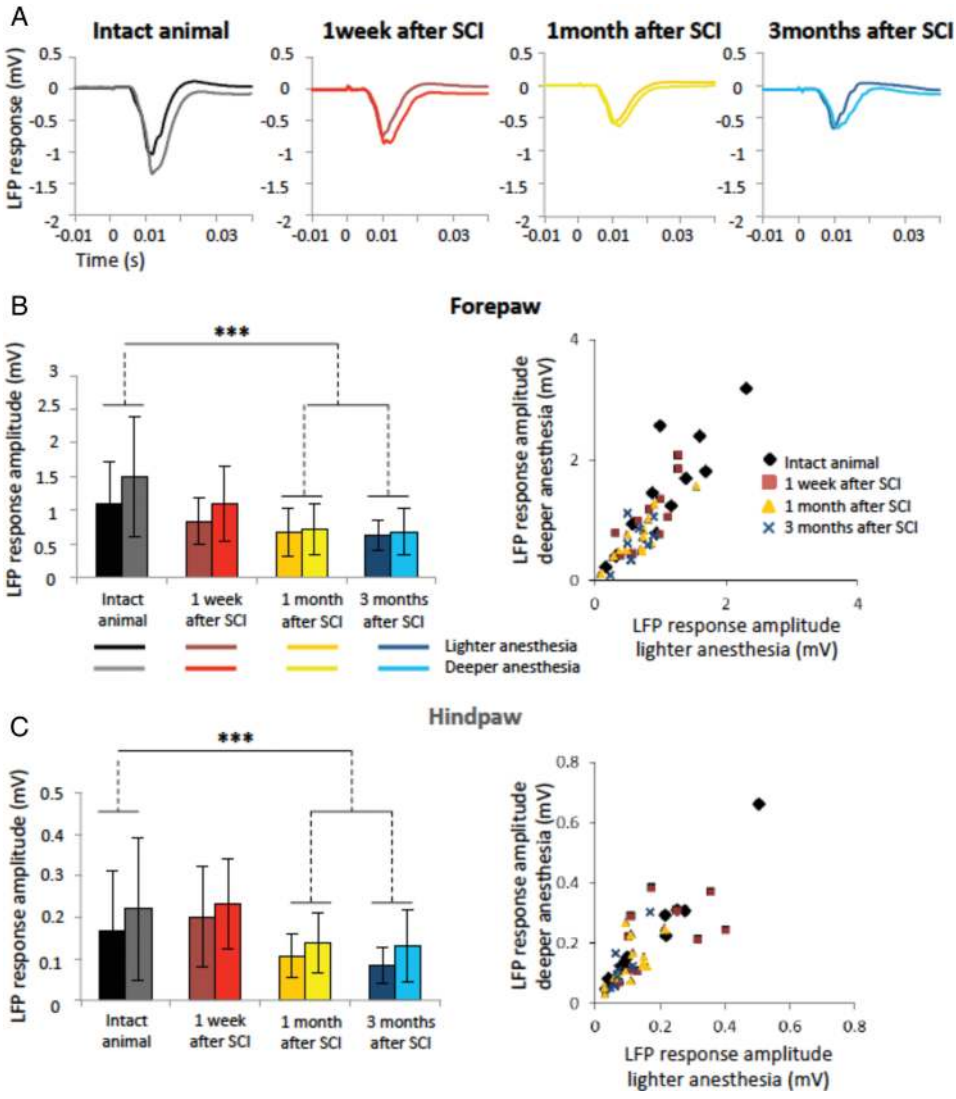

Figure 2. Decreased cortical responses after thoracic spinal cord transection. (*A*) Grand average of LFP responses evoked by high-intensity (5 mA) stimuli delivered to the contralateral forepaw in the different groups of animals, under lighter anesthesia (darker color) and deeper anesthesia (lighter color). (*B–C*) Corresponding measures of the response amplitude in the forepaw (*B*) and hindpaw cortex (*C*). (Left) Bars represent the means and the error bars are the standard deviations. (Right) Scatter plots of all the data. Each point represents the LFP amplitude of a single animal under lighter (*x*-axis) and deeper anesthesia (*y*-axis): $^{*}P < 0.05$; $^{**}P < 0.01$; $^{***}P < 0.001$.

cortex and in the adjacent forepaw cortex separately, as well as the responses evoked in the forepaw cortex by low-intensity forepaw stimuli (0.5 mA: interaction TIME × STIMULATION $F_{6,229} = 2.2$, $P = 0.0484$). Note that the responses evoked in the hindpaw cortex by low-intensity forepaw stimuli were not quantified due to their inconsistency in our experimental conditions (see also Morales-Botello et al. 2012). The long-term "*decrease*" in fast cortical responsiveness after TX was not only observed for the responses evoked by high-intensity forepaw stimuli in the deafferented hindpaw cortex (follow-up 2-way independent-measures ANOVA, TIME $F_{3,75} = 4.6$, $P = 0.0054$), but also in the adjacent forepaw cortex ($F_{3,77} = 5.7$, $P = 0.0012$). This similarity is not particularly surprising, for 2 reasons: (1) the forepaw cortex of intact animals consistently responds to hindpaw stimuli (Moxon et al. 2008; Aguilar et al. 2010; Morales-Botello et al. 2012; Humanes-Valera et al. 2013; Yague et al. 2014), therefore the supposedly intact forepaw cortex would also be partially deafferented after thoracic SCI and this could explain the long-term decrease in fast cortical responses observed here; (2) recent anatomical data suggested that GABAergic tone is enhanced in the forepaw cortex after thoracic SCI (Orlando and Raineteau 2015). Interestingly, the decrease in fast cortical responsiveness after TX was not significant for the responses evoked by low-intensity forepaw stimuli (0.5 mA: $F_{3,77} = 2.1$, $P = 0.11$), which is consistent with the absence of spontaneous cortical reorganization previously reported when tested with mild mechanical stimuli (Jain et al. 1995; Graziano et al. 2013), as well as with the absence of behavioral changes in forepaw tactile sensation in the same model of SCI (M'Dahoma et al. 2014). A long-term decrease in fast cortical responses to forepaw stimuli after TX may therefore only be apparent when tested with stimuli that are sufficiently strong to fully engage cortical circuits. Hence, we subsequently focused on cortical responses to high-intensity stimuli. Furthermore, as the smaller responses were virtually identical 1 month and 3 months after TX (Fig. 2), these 2 groups of animals were pooled together.

The Long-term Decrease in the Fast Cortical Responses to Forepaw Stimuli After TX Probably Reflects Synaptic Pruning

The diminished fast cortical responses to forepaw stimuli observed 1–3 months after TX could be the functional consequence of synaptic pruning. To support this hypothesis, a few alternative mechanisms that could also provoke a similar dampening of cortical responsiveness to forepaw stimuli must first be excluded. Three alternative explanations were considered: (1) a classic forepaw-to-hindpaw shift in cortical focus; (2) a gross increase in spontaneous cortical activity; (3) a loss of the cortical network activity underlying higher responsiveness to stimuli that might occur during down-states rather than up-states.

The first possible explanation for the smaller fast cortical responses is that of a classical expansive reorganization, with a shift of the forepaw cortical representation toward the deafferented hindpaw area (Endo et al. 2007; Ghosh et al. 2010). This explanation is highly unlikely because it would imply an increase in the responses evoked in the hindpaw cortex by forepaw stimuli. However, the responses evoked by high-intensity forepaw stimuli 1–3 months after TX were smaller than those in intact animals both in the forepaw and the hindpaw cortex. Therefore, the observed long-term decrease in fast cortical responses to forepaw stimuli after TX is not secondary to a shift of the forepaw cortical representation towards the deafferented hindpaw area. Previous imaging data also seem to exclude a possible shift of the forepaw cortical representation in the antero-posterior direction (Endo et al. 2007; Ghosh et al. 2010).

A second possible explanation for the smaller fast cortical responses to forepaw stimuli 1–3 months after TX could be a gross increase in cortical spontaneous activity, that is, the exact opposite of what occurs immediately after the lesion (Aguilar et al. 2010). The rationale behind this alternative explanation is provided by the well-known state dependency of cortical somatosensory responses (Petersen et al. 2003; Sachdev et al. 2004; Hasenstaub et al. 2007; Reig and Sanchez-Vives 2007; Aguilar et al. 2010; Humanes-Valera et al. 2013). To exclude this explanation, we investigated the cortical spontaneous activity measured as the average rectified rMUA, a very sensitive measure in our experience (Aguilar et al. 2010, 2011; Humanes-Valera et al. 2013; Yague et al. 2014). We observed a different pattern of spontaneous activity in the forepaw cortex than in the hindpaw cortex (3-way independent-measures ANOVA, interaction TIME × CORTEX $F_{3,154} = 4.2$, $P = 0.0071$; Fig. 3A,B). Specifically, in the forepaw cortex we found the expected experimental difference between deep and light anesthesia in all animal groups (2-way independent-measures ANOVA, ANESTHESIA $F_{1,79} = 30.3$, $P < 0.0001$), and the level of cortical spontaneous activity was similar in animals recorded 1 week or 1–3 months after TX with respect to the intact animals (TIME $F_{2,79} = 1.5$, $P = 0.22$; interaction TIME × ANESTHESIA $F_{2,79} = 0.003$, $P = 0.996$). Conversely, while the expected difference between deeper and lighter anesthesia was also seen in the hindpaw cortex in all groups of animals (ANESTHESIA $F_{1,79} = 33.1$, $P < 0.0001$), the cortical spontaneous activity under lighter anesthesia—but not under deeper anesthesia—was lower rather than higher in animals recorded 1 week or 1–3 months after TX relative to the intact animals (TIME × ANESTHESIA $F_{2,79} = 4.7$, $P = 0.0116$; Tukey: $P < 0.0038$). Accordingly, we are confident that the long-term decrease in fast cortical responses was not secondary to a gross increase in cortical spontaneous activity. Rather, the long-term decrease in cortical spontaneous activity in the hindpaw cortex after TX is consistent with the postulated loss of cortical synapses (Ghosh et al. 2012), as well as with decrease in the tonic thalamocortical inputs from the deafferented hindpaw (Rigas and Castro-Alamancos 2007; Hirata and Castro-Alamancos 2010; David et al. 2013).

The third and most complicated of the alternative explanations for the long-term decrease of fast cortical responses to forepaw stimuli is suggested subtly by our own data. The attentive reader might have noticed that LFP responses were larger in intact animals under deep anesthesia compared with light anesthesia, yet not 1–3 months after TX (Fig. 2A,B). This could be due to alterations of the cortical network mechanisms underlying higher responsiveness to somatosensory stimuli occurring during down-states compared with up-states (Petersen et al. 2003; Sachdev et al. 2004; Hasenstaub et al. 2007; Reig and Sanchez-Vives 2007; Aguilar et al. 2010; Humanes-Valera et al. 2013). To exclude this possibility, we reanalyzed the data on a single-trial basis. We focused specifically on the relationship between the spontaneous activity immediately before each stimulus—measured as the mean rMUA in the 45 ms pre-stimulus—and the amplitude of the corresponding single-trial LFP response (Aguilar et al. 2010; Humanes-Valera et al. 2013). The tight negative correlation between pre-stimulus rMUA and single-trial LFP response observed in intact animals (Pearson $R < -0.82$, $n = 100$ trials) was preserved after SCI ($R < -0.89$), confirming that the cortical network mechanisms underlying higher responsiveness to stimuli occurring during down-states was maintained and could not explain the observed decrease in fast cortical responses. In fact, the LFP responses in animals recorded 1–3 months after TX were smaller than those in intact animals for all levels of prestimulus spontaneous activity. Importantly, 1–3 months after TX the slope of the relationship between prestimulus rMUA and single-trial LFP response was less steep under lighter anesthesia compared with deeper anesthesia (Fig. 3C). This observation is important for two reasons: (1) it explains why the average LFP responses observed 1–3 months after TX were similar under lighter and deeper anesthesia (Fig. 2A,B); (2) it suggests that cortical adaptation may be worse 1–3 months after TX than in intact animals, a possibility that was investigated further (see below).

Overall, synaptic pruning represents the most likely explanation for the long-term decrease in fast cortical responses to forepaw stimuli 1–3 months after TX.

Intracellular Correlates of Decreased Fast Cortical Responses After TX

In order to integrate the information obtained at the population level with that at the cellular level, we performed in vivo intracellular recordings in the deafferented hindpaw infragranular somatosensory cortex in intact animals ($n = 11$ cells from 8 animals), immediately after TX ($n = 10$ cells from 5 of the above 8 animals), and in animals 1–3 months after TX ($n = 10$ cells from 4 rats). Note that even though the immediate effects of cortical reorganization after TX were characterized extracellularly in our previous works (Aguilar et al. 2010; Humanes-Valera et al. 2013), this time period is included here to provide the complete intracellular dataset (as far as we know these are the first cortical intracellular recordings reported in the literature after SCI). All cells but 2 were physiologically identified as putative pyramidal neurons (Fig. 4A) and all the intracellular measures were obtained during the down-states.

Our data suggest that TX did not have a strong impact on the basic intrinsic properties of the cells (Fig. 4B,C), as the resting membrane potential did not increase significantly immediately after TX (one-way ANOVA $F_{2,27} = 2.6$, $P = 0.0896$), while the

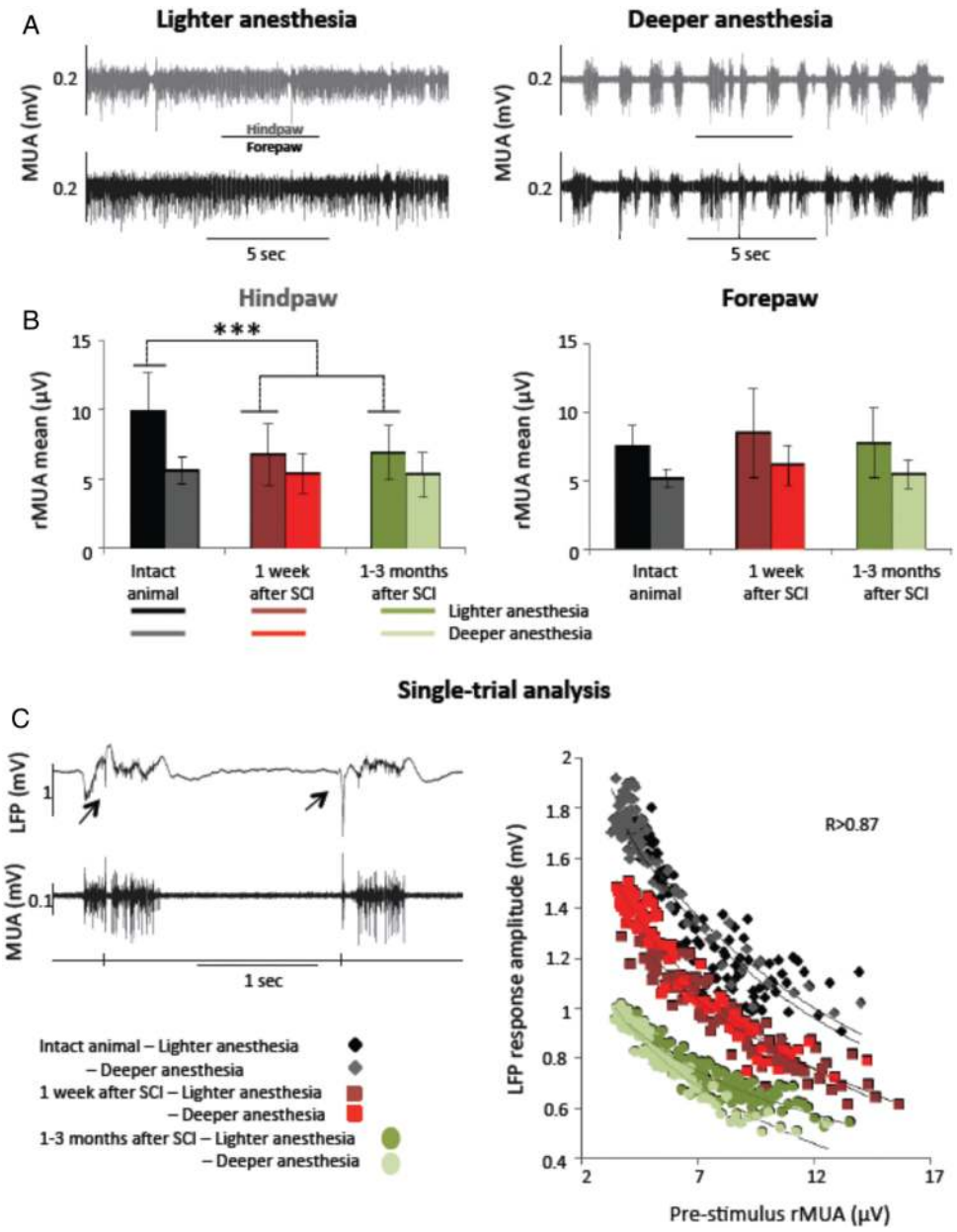

Figure 3. Spontaneous activity and single-trial analysis. (*A*) Representative examples of spontaneous MUA simultaneously recorded in the hindpaw cortex (gray) and forepaw cortex (black) under lighter (left) and deeper anesthesia (right). (*B*) Average rectified multiunit activity (rMUA) in the hindpaw (left) and forepaw cortex (right). Bars represent the means and the error bars are the standard deviations: $^{*}P < 0.05$; $^{**}P < 0.01$; $^{***}P < 0.001$. (*C*) (Left) Representative LFP (upper trace) and MUA recordings (lower trace) around 2 single-trial stimuli delivered in the up and down cortical states. (Right) Joint single-trial analysis of spontaneous activity (mean rMUA in the 45 ms prestimulus, x-axes) and the responses evoked in the forepaw cortex by high-intensity forepaw stimuli (LFP amplitude, y-axes). Single trials were sorted within animals based on the prestimulus rMUA and then averaged across the animals in each group. Best-fitting exponential curves are also shown for each group.

membrane resistance was indistinguishable in the 3 groups ($F_{2,25} = 0.1$, $P = 0.88$). Conversely, TX had a strong impact on the synaptic responses to high-intensity forepaw stimuli, as expected from the LFP results (Fig. 4*D*–*G*). Indeed, the amplitude of synaptic responses was significantly higher than in intact animals immediately after TX ($F_{2,27} = 6.5$, $P = 0.0050$; unpaired one-sided *t*-test: $P = 0.0085$) and significantly smaller 1–3 months after TX than immediately after TX ($P = 0.0013$), although this amplitude was not significantly smaller than that in intact animals ($P = 0.14$). Similarly, the slope of the synaptic responses tended to be higher immediately after TX compared with intact animals ($F_{2,27} = 6.2$, $P = 0.0060$; unpaired one-sided *t*-test: $P = 0.10$) and it was significantly smaller 1–3 months after TX when compared with the slope both immediately after TX ($P = 0.0045$) and in intact animals ($P = 0.0152$). These results suggest that the immediate increase in LFP responses reported previously (Humanes-Valera et al. 2013), and the long-term decrease in LFP responses 1–3 months after TX reported here, represent the population effects of synchronous synaptic responses at the cellular level.

Long-term Decrease in the Adaptation of Fast Infragranular Cortical Responses After TX

According to basic neurophysiology, proximal synaptic inputs—those closer to the soma—induce steeper synaptic responses

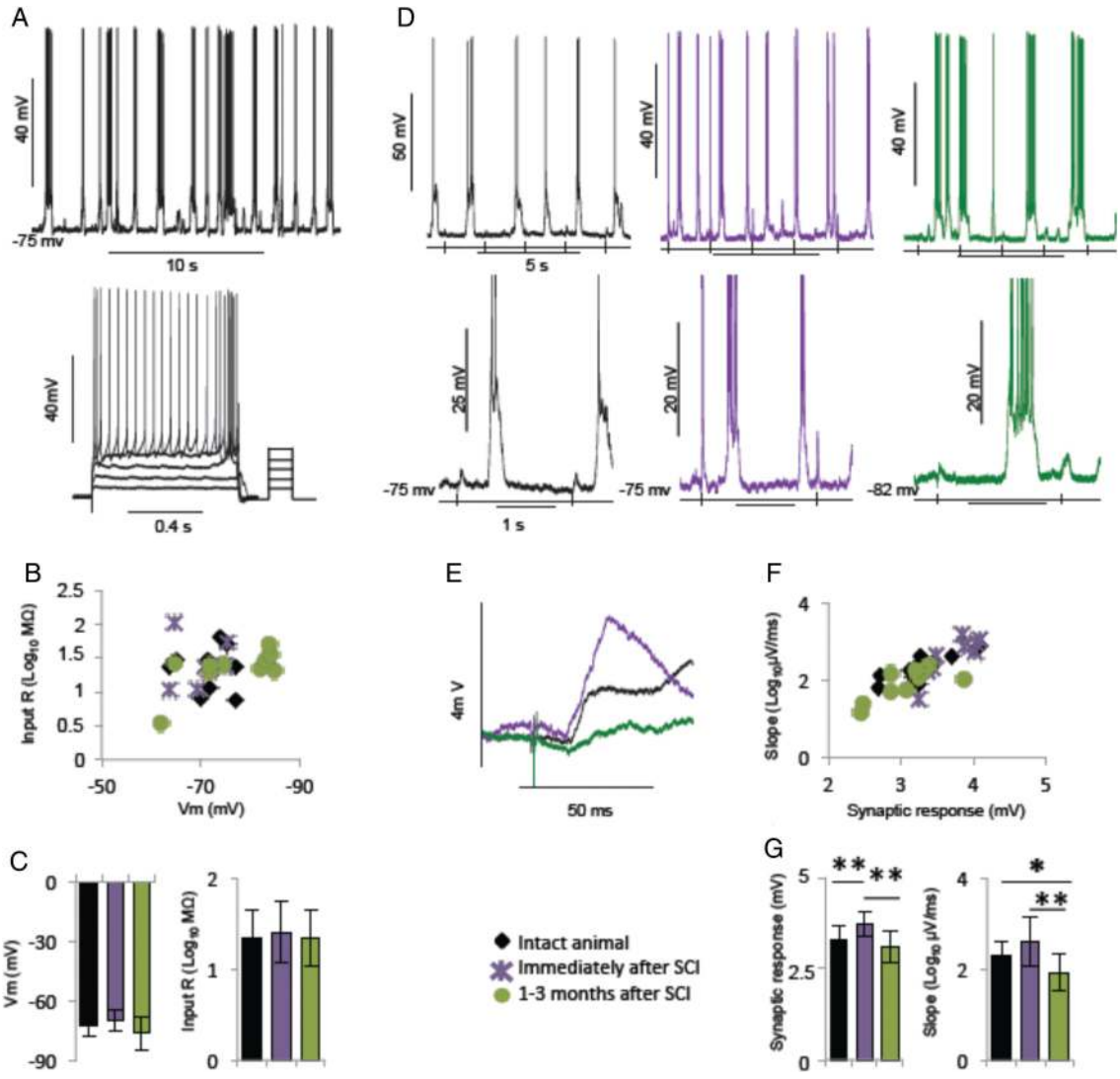

Figure 4. Intracellular recordings. (*A*) Representative cell recorded in the infragranular hindpaw cortex during spontaneous activity (above) and in response to current pulses (below). (*B*) Scatter plot of the resting membrane potential (V_m, x-axis) and input resistance (*R*, y-axis) of all cells recorded in 3 different groups of animals: intact (black), immediately after injury (purple), and 1–3 months after injury (green). (*C*) Corresponding average measures. (*D*) Representative intracellular recordings in the infragranular hindpaw cortex during consecutive forepaw stimuli (5 stimuli above, 2 stimuli expanded below) in the 3 groups of animals. (*E*) Grand average of synaptic responses. (*F*) Scatter plot of the amplitude (x-axis) and slope (y-axis) of the synaptic responses in all cells. (*G*) Corresponding average measures. The bars represent the means and the error bars are the standard deviations: $^*P < 0.05$; $^{**}P < 0.01$; $^{***}P < 0.001$.

compared with distal synaptic inputs. Therefore, the more gentle slope of the synaptic responses observed 1–3 months after TX is consistent with a greater loss of proximal synapses in the infragranular cortex compared with the distal synapses in the supragranular cortex. In keeping with this view, cortical spine loss after SCI seems to be more severe in the infragranular layers compared with the supragranular layers (Ghosh et al. 2012). This difference is particularly relevant from a functional perspective, given that thalamo-cortical synapses have opposing physiological properties in infragranular and supragranular layers (Viaene et al. 2011a; 2011b). Infragranular cells produce mostly "Class 1" responses to thalamic inputs characterized by paired-pulse adaptation (Viaene et al. 2011a), while supragranular cells produce mostly "Class 2" responses characterized by paired-pulse facilitation (Viaene et al. 2011b). Therefore, we predicted that the stronger loss of infragranular rather than supragranular synapses after TX would reduce the adaptation of infragranular LFP responses to repetitive forepaw stimuli.

In order to test this prediction, we recorded infragranular LFP responses to 10 Hz trains of 10 stimuli delivered to the contralateral forepaw in a subset of animals (intact, $n = 9$; 1–3 months after TX, $n = 17$). Accordingly, our data show that paired-pulse adaptation (the response amplitude ratio between the second and first stimulus of the train, i.e., second/first) was weaker in animals recorded 1–3 months after TX compared with intact animals, that is, the response amplitude ratio was closer to one (3-way ANOVA, TIME $F_{1,144} = 4.68$, $P = 0.0254$: Fig. 5A). Within the context of synaptic depression, decreased cortical adaptation might intuitively be considered as an obvious consequence of decreased cortical responsiveness. However, this was not the case and in fact, in the whisker system it has been elegantly shown how and why weaker stimuli produce "more" cortical adaptation than stronger stimuli (Ganmor et al. 2010; Mohar et al. 2013). Indeed, our data confirm and extend these findings to the hindpaw–forepaw cortex, in which paired-pulse adaptation was nicely dependent on stimulation (STIMULATION $F_{2,144} = 21.35$, $P < 0.0001$), being

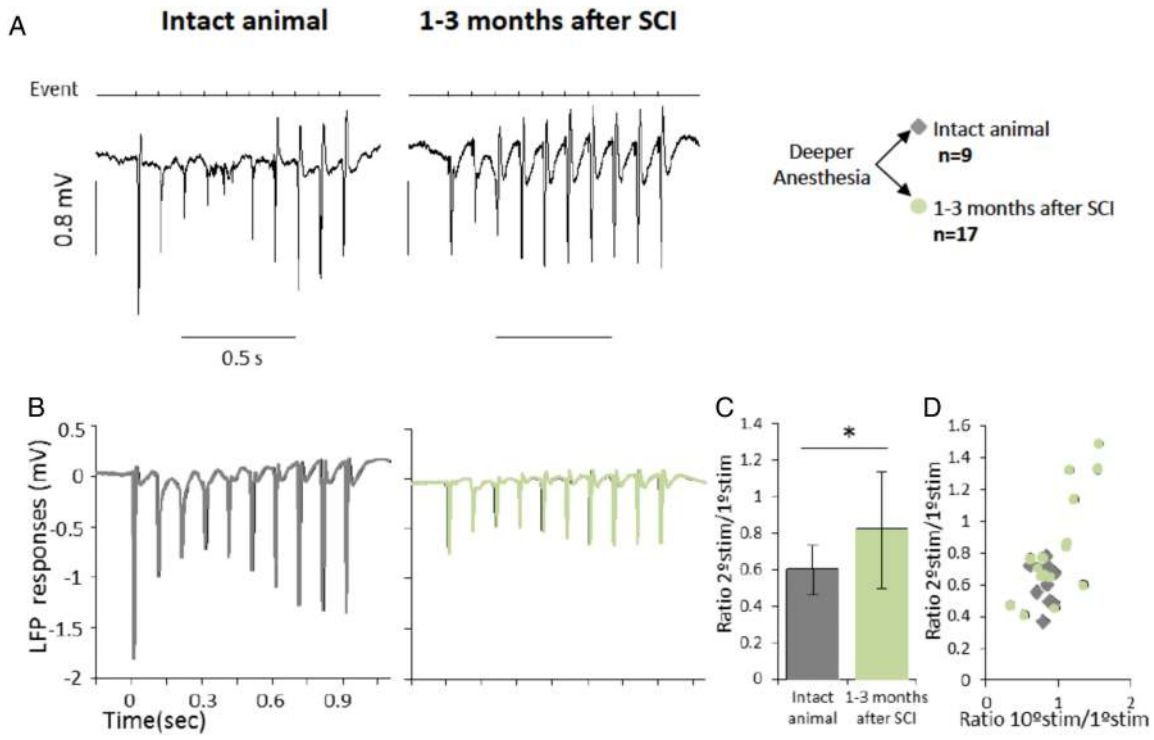

Figure 5. Cortical adaptation decreases after thoracic spinal cord transection. (*A*) Raw traces with representative single-trial LFP responses evoked by 10 Hz stimulus trains of high intensity (5 mA) stimuli delivered to the contralateral forepaw in an intact animal (left) and in an animal recorded 1 month after SCI (right). (B) Corresponding grand-averages—across all trials and all animals—in intact animals (gray, left) and in animals recorded 1–3 months after SCI (green, right). (C) Corresponding average measures of paired-pulse adaptation, that is, the response amplitude ratio between the second and the first stimulus of the train (second/first). An amplitude ratio closer to one indicates less adaptation. The bars represent the means and the error bars the standard deviations. *$P < 0.05$ (*D*) Scatter plot of paired-pulse adaptation (*y*-axis) versus steady-state adaptation (*x*-axis) for all animals.

weaker in response to high-intensity than low-intensity forepaw stimuli (Tukey: $P = 0.0003$), and even lower when the responses to high-intensity forepaw stimuli were recorded in the hindpaw cortex than in the forepaw cortex ($P = 0.0099$). Thus, the decreased cortical adaptation is not an obvious consequence of the decreased cortical responsiveness, but rather a genuine functional aspect of long-term cortical reorganization after SCI. As expected, paired-pulse adaptation was stronger under deeper anesthesia compared with lighter anesthesia (STATE $F_{1,144} = 18.82$, $P < 0.0001$), consistent with classical studies in the whisker cortex (Castro-Alamancos 2004b).

Steady-state adaptation, measured as the response amplitude ratio between the tenth and first stimulus of the train (tenth/first), yielded similar results. Thus, there was a tendency toward stronger adaptation during deep rather than light anesthesia (STATE $F_{1,\ 143} = 3.2725$, $P = 0.0725$), while adaptation was weaker for high-intensity stimuli than for low-intensity stimuli (STIMULATION $F_{2,\ 143} = 57.33$, $P = 0.0001$). Most importantly, weaker adaptation was observed in animals recorded 1–3 months after TX than in intact animals (TIME $F_{1,\ 143} = 4.71$, $P = 0.0317$).

These results show that the electrophysiological characterization of long-term cortical reorganization after SCI is not limited to the long-term decrease of infragranular responsiveness, but also involves a long-term decrease in infragranular adaptation.

The Long-term Decrease in Fast Cortical Responses co-exists with an Increase in Slow Cortical Activation After TX

So far we have provided electrophysiological evidence of the long-term cortical reorganization that occurs after SCI, involving reduced responsiveness and adaptation in the infragranular somatosensory cortex, which is consistent with the anatomical evidence of infragranular synaptic pruning after TX (Ghosh et al. 2012). However, in order to establish a complete electrophysiological framework of the long-term cortical reorganization after SCI, we need to reconcile our results with the long-term increase in cortical responsiveness observed after TX with fMRI recordings (Endo et al. 2007; Ghosh et al. 2010). Due to the slower nature of fMRI responses, we sought electrophysiological evidence for the long-term increases in cortical excitability after TX over slower timescales post-stimulus, both at the population and cellular levels.

At the population level, we previously described that when the cortex is in a state of slow-wave activity, there are 2 components to the responses evoked in the hindpaw cortex by forepaw stimuli: (1) faster short-latency responses (<30 ms) typical of the thalamocortical responses (Manns et al. 2004), and (2) slower long-latency activations (>50 ms) that correspond to up-states triggered in the forepaw cortex that propagate to the hindpaw cortex (Castro-Alamancos 2009; Aguilar et al. 2010; Humanes-Valera et al. 2013). Therefore, we quantified these slower long-latency activations for each stimulation protocol in terms of probability that the stimuli delivered to the forepaw triggered up-states in the hindpaw cortex (Fig. 6A). With high-intensity stimuli, the probability of observing stimulus-triggered up-states in the hindpaw cortex was close to 100%. In contrast, with low-intensity stimuli this probability was much lower and, importantly, it was significantly higher in animals recorded 1–3 months after TX than in intact animals (2-way ANOVA, interaction TIME × CORTEX $F_{1,30} = 15.8$, $P = 0.0004$; Tukey: $P = 0.0002$; Fig. 6B,C). Furthermore, the probability of

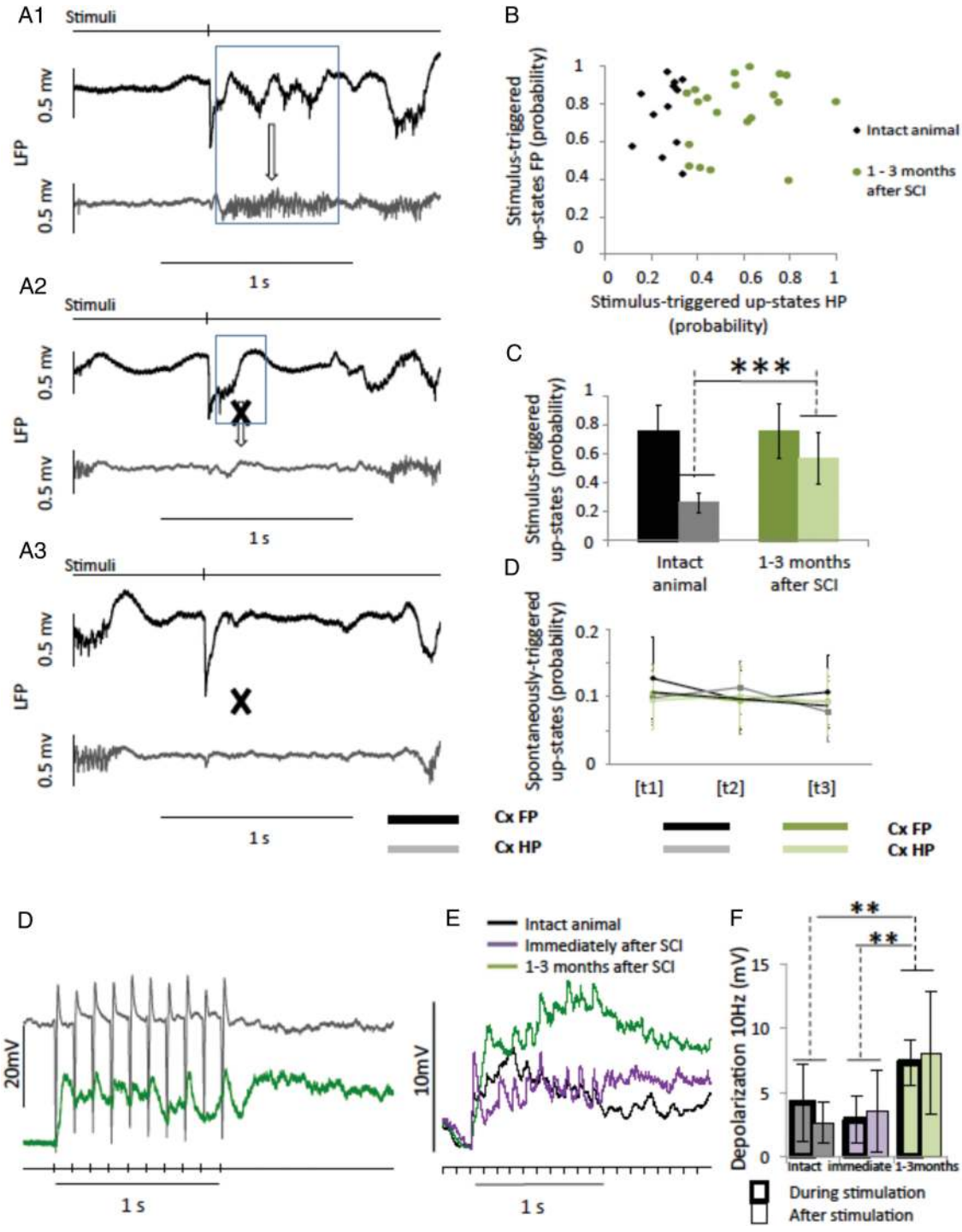

Figure 6. Increased cortical responses over slower timescales. (*A*) Three representative examples of LFP responses evoked in the forepaw (Cx FP, black) and hindpaw cortex (Cx HP, gray) by low-intensity (0.5 mA) forepaw stimuli. The examples are single trials in which the stimulus triggered an up-state in the forepaw cortex that propagated to the hindpaw cortex (A1), the stimulus triggered an up-state in the forepaw cortex that did not propagate to the hindpaw cortex (A2), or the stimulus did not trigger an up-state in either cortex (A3). (*B*) Scatter plot representing the probability of up-states being triggered in the hindpaw (*x*-axis) and forepaw cortex (*y*-axis) by forepaw stimuli in intact animals (black) and in animals recorded 1–3 months after SCI. Each point corresponds to an individual animal. (*C*) Corresponding measures of stimulus-triggered up-states. The bars represent the means and the error bars are the standard deviations: ***$P < 0.001$. (*D*) Spontaneously triggered up-states −200 to 0 ms before each stimulus [t1], 500–700 ms after each stimulus [t2]; and 1000–1200 ms after each stimulus [t3]. (*E*) Representative LFP recording from the forepaw cortex (upper trace) and intracellular recording in hindpaw cortex (lower trace) in response to 10 Hz forepaw stimuli. (*F*) Grand average of the membrane potential responses of cells recorded in intact animals (black line), immediately after injury (purple line) and 1–3 months after injury (green line). (*G*) Corresponding measures of slow sustained depolarization. The bars represent the means, the error bars are the standard deviations and the asterisks indicate significant differences: **$P < 0.01$.

observing stimulus-triggered up-states in the forepaw cortex was no different 1–3 months after TX than in intact animals ($P > 0.99$). As a control analysis, we verified that the increased probability of observing stimulus-triggered up-states in the hindpaw cortex was not due to an increase probability of observing spontaneously-triggered up states 1–3 months after TX (3-way ANOVA, $P > 0.28$; Fig. 6*D*). These results suggest that at the population level it is possible to electrophysiologically detect a long-term increase in cortical activation over slow time scales (>50 ms) due to the long-term increase in cortico-cortical propagation of stimulus triggered up-states after SCI.

At the cellular level, repetitive 8 Hz whisker stimulation in mice induces slow sustained depolarizations in cortical neurons that are responsible for long-term potentiation (LTP) (Gambino et al. 2014). A subset of the cells recorded intracellularly in the hindpaw cortex ($n = 10$ in intact animals; $n = 7$ in animals recorded immediately after TX; $n = 6$ in animals recorded 1–3 months after TX) were subjected to the 10-Hz stimulation protocol used to quantify adaptation. However, the synaptic responses were too small and variable (particularly 1–3 months after TX) to quantify robust paired-pulse adaptation in the deafferented hindpaw cortex. Nevertheless, the 10 Hz stimulus trains (at 5 mA) induced responses that involved slow-rising and long-lasting depolarizations (typically subthreshold), which slowly decayed at the end of the stimulus train (Fig. 6*E–G*). These slow sustained depolarizations were remarkably similar to the depolarizations reported with 8 Hz whisker stimulation (Gambino et al. 2014). We did not observe any sustained firing in the MUA of our extracellular recordings, consistent with the subthreshold nature of these depolarizations (data not shown). Importantly, these slow sustained depolarization were similar in cells recorded immediately after TX to those from intact animals, yet they were surprisingly higher in cells recorded 1–3 months after TX (2-way ANOVA, TIME $F_{2,20} = 8.4$, $P = 0.0022$; Tukey $P = 0.0047$ compared with immediately after TX, and $P = 0.0041$ compared with intact animals; Fig. 6*G*). It remains to be established whether these slow sustained depolarizations could also be elicited by stimulation amplitudes and frequencies relevant to fMRI protocols (1 mA at 3 Hz in Endo et al. 2007; 1.6–6 mA at 3 Hz in Ghosh et al. 2010). Nevertheless, these data show that at the cellular level it is also possible to electrophysiologically reveal an increase in cortical activation at slow post-stimulus timescales.

Discussion

In this work, we demonstrate that 1–3 months after complete thoracic spinal cord transection a striking decrease in fast cortical responses to high-intensity forepaw stimuli is produced in conjunction with an increase in cortical activation over slower post-stimulus time scales. The long-term decrease in fast cortical responses was observed at both the population level (through decreased LFP responses) and the intracellular level (as dampened synaptic responses). Likewise, the long-term increase in slow cortical activation was also observed at the population level (through enhanced forepaw-to-hindpaw propagation of stimulus-triggered up-states), and at the intracellular level (through increased slow sustained depolarization evoked in the deafferented hindpaw cortex by high-frequency forepaw stimuli). Decreased and increased cortical responsiveness can therefore coexist over different post-stimulus time scales, providing a dual electrophysiological framework of cortical reorganization after SCI.

Early versus Long-term Cortical Reorganization After SCI

Our framework reconciles several conflicting observations in the literature regarding reorganization of the somatosensory cortex after SCI. It is important to remark that we are referring to lesioned animals that did not receive any exercise, pharmacological therapies, or other interventions that affect cortical reorganization after SCI. Integrating the present findings with previous results, we can define a time course of cortical reorganization after complete SCI in rats that involves at least 2 phases: an early phase, minutes-to-days after injury; and a more long-term phase, weeks-to-months after injury.

In the early phase, increased cortical responses to high-intensity stimuli above the level of the lesion are observed over fast post-stimulus time scales (i.e., tenths of ms post-stimulus). These responses are evident both in the infragranular layers, through extracellular (Aguilar et al. 2010; Humanes-Valera et al. 2013) and intracellular recordings (data herein), and in the supragranular layers, through voltage-sensitive dye imaging (Ghosh et al. 2010). In the same early phase, increased cortical activation can also be observed over slower time scales (i.e., hundreds of ms) when measured by fMRI (Endo et al. 2007; Ghosh et al. 2010; Sydekum et al. 2014). Therefore, there is substantial agreement that in the early phase of cortical reorganization after SCI cortical responsiveness increases over all time scales, leading to classical expansive reorganization.

Conversely, in the long-term there is a decrease in cortical responses to high-intensity stimuli above the level of the lesion over fast time scales, as witnessed here. This long-term decrease in fast cortical responses is consistent with the absence of long-term cortical reorganization observed from single-unit responses to mild tactile stimuli in untreated rats after SCI (Jain et al. 1995; "sham" animals in Graziano et al. 2013). In the same late phase, increased cortical activation can be observed over slower time scales, as measured by fMRI (Endo et al. 2007; Ghosh et al. 2010), through the forepaw-to-hindpaw propagation of stimulus-triggered up-states in population recordings, and through slow sustained depolarizations in intracellular recordings. It is important to note that fMRI metabolic responses are typically obtained at 3 Hz with high-intensity stimuli (≥1 mA), which are likely to induce slow subthreshold depolarization. This suggests that the stronger fMRI responses might reflect the increased metabolic activity that is related to the increased slow subthreshold depolarizations reported here. In any case, our data show that increased and decreased cortical responsiveness can coexist in different post-stimulus timescales within the long-term phase of cortical reorganization after SCI.

Mechanism(s) of Long-term Cortical Reorganization After SCI

Synaptic pruning represents the most plausible mechanism underlying the long-term decrease in fast cortical responses reported here after spinal cord transection (Kim et al. 2006; Ghosh et al. 2012; Zhang et al. 2015). The loss of infragranular synapses is likely to lead to the observed combination of a decrease in amplitude and slope of synaptic potentials at the intracellular level, ultimately producing the decreased responsiveness at the population level. In support of this hypothesis, we excluded 3 alternative mechanisms that could also lead to decreased cortical responsiveness: a classical forepaw-to-hindpaw shift in cortical focus; a gross increase in cortical spontaneous activity; and a loss of the cortical network activity underlying greater responsiveness to stimuli occurring during down-states as opposed to up-states. The link between decreased fast cortical responses and pruning is further supported by a more sophisticated corollary prediction that arises from the layer-specificity of synaptic pruning after SCI. Infragranular neurons lose spines specifically

in the dendritic segment proximal to the soma, corresponding to layer 5, and to a much lesser extent in the distal segment corresponding to layers 2/3 (Ghosh et al. 2012). Thalamocortical inputs to layer 5 are mainly characterized by paired-pulse adaptation (Viaene et al. 2011a), whereas paired-pulse facilitation is the main characteristic of thalamocortical inputs to layer 2/3 (Viaene et al. 2011b). It therefore follows that a greater loss of infragranular as opposed to supragranular synapses should shift the paired-pulse behavior of infragranular neurons from adaptation towards facilitation. This prediction is confirmed by the weaker adaptation to 10 Hz stimuli observed in animals 1–3 months after SCI. It should be noted that this weaker cortical adaptation cannot simply be due to decreased cortical responsiveness, since low-intensity stimuli produced more cortical adaptation in our experiments than high-intensity stimuli, consistent with previous observations in the whisker system (Ganmor et al. 2010; Mohar et al. 2013). Although we cannot exclude a contribution of altered noradrenergic and/or cholinergic neuromodulatory systems (Favero et al. 2012; Castro-Alamancos and Gulati 2014), reduced infragranular cortical adaptation could be a genuine functional consequence of layer-specific infragranular pruning.

The possible mechanisms underlying the increase in slow cortical activation are somewhat more complex. At the intracellular level, we observed an increase in slow sustained depolarizations in response to stimulus trains in animals recorded 1–3 months after SCI. These increased depolarizations could simply be another electrophysiological consequence of the layer-specificity of synaptic pruning at the dendritic segment proximal to the soma (Ghosh et al. 2012), whereby the slower dynamics of metabotropic receptors (Viaene et al. 2011a) and plateau potentials (Gambino et al. 2014) in the distal supragranular segment become predominant in the overall subthreshold activity of infragranular neurons (Breton and Stuart 2009). At the population level, we observed an increased probability of stimulus-triggered up-states propagating from the forepaw cortex to the hindpaw cortex 1–3 months after SCI. According to previous work on the barrel cortex in vitro (Wester and Contreras 2012), layer 5 is critical for the propagation of up-states and therefore, one would expect infragranular pruning to diminish rather than enhance the probability of stimulus-triggered up-states propagating from the forepaw to hindpaw cortex, the opposite of what we found. One possible explanation is that infragranular pruning after SCI might affect vertical/local connectivity more intensely (Feldmeyer 2012) than horizontal/global connectivity (Schnepel et al. 2015). Such dissociation between local and global connectivity has already been observed in other models of deafferentation (Butz et al. 2014). An additional explanation is that SCI might induce long-term alterations to neuromodulatory systems, and in particular, a reduction of cholinergic tone would increase the cortico-cortical propagation of up-states (Wester and Contreras 2012). We showed previously that acute SCI slows down spontaneous cortical activity (Aguilar et al. 2010; Yague et al. 2014) and decreases the requirements for anesthesia (Foffani et al. 2011). Here, slower spontaneous activity was still evident in the deafferented cortex 1–3 months after SCI, which could indeed be a consequence of cholinergic depression. We also cannot rule out whether increased cortico-cortical propagation of stimulus-triggered up-states reflects classical cortico-cortical rewiring. Whatever the exact mechanisms, the coexistence of decreased fast cortical responsiveness and increased slow cortico-cortical up-state propagation observed here suggests that long-term cortical reorganization after SCI might involve an elegant combination of dampened vertical/local connectivity and enhanced horizontal/global connectivity.

Pathophysiological Implications

Our findings have several possible pathophysiological implications. First, the coexistence of different effects on different post-stimulus time scales offers a dual framework not only for reconciling results obtained with different techniques in the same animal models (e.g., electrophysiology vs. fMRI), but also for carefully translating the results from animals models to human patients. In this respect, it is important to remark the lack of a complete segregation between forepaw and hindpaw representation in the rat somatosensory cortex (Moxon et al. 2008; Aguilar et al. 2010; Morales-Botello et al. 2012; Humanes-Valera et al. 2013; Yague et al. 2014). Second, the equilibrium between decreased vertical/local connectivity and increased horizontal/global connectivity might be critical for the appearance of classical expansive reorganization. In this regard, it is important to note that complete spinal cord transection—the same model used here—alters the transcriptional activity of genes and the protein expression associated with cortical plasticity (Endo et al. 2007; Graziano et al. 2013). Therapies that boost cortical plasticity, such as exercise (Kao et al. 2009; Jones et al. 2009; van den Brand et al. 2012; Graziano et al. 2013; Oza and Giszter 2014, 2015), serotonergic pharmacotherapy (Ganzer et al. 2013; Foffani et al. 2016), or simply environmental enrichment (Kim et al. 2008), might favor increased horizontal/global connectivity over decreased vertical/local connectivity, ultimately inducing classical expansive reorganization. This therapy-dependent switch from reduced responsiveness to expansive reorganization should be carefully considered when relating our results—obtained in unexercised, untreated animals in a somatosensory context—to motor cortex reorganization with and without exercise of various kinds after SCI (Fouad et al. 2001; van den Brand et al. 2012; Oza and Giszter 2014, 2015; Ganzer et al. 2016) or to other deafferentation effects observed in motor contexts (Sanes and Donoghue 2000). Finally, the same equilibrium could be determinant for the trade-off between adaptive reorganization, promoting behavioral recovery (Manduch et al. 2002; Curt et al. 2002; Cramer et al. 2005; Lotze et al. 2006; Hoffman and Field-Fote 2010), and maladaptive reorganization, leading to neuropathic pain (Flor et al. 1995; Lotze et al. 1999; Peyron et al. 2004; Wrigley et al. 2009a; 2009b; Gustin et al. 2012; Makin et al. 2013). Our results add 1 degree of freedom, suggesting that fast cortical responses and slow cortical activation might be affected distinctly in different deafferentation models, and targeted separately by different therapeutic approaches. Thanks to this additional degree of freedom, our dual framework supports a critical functional role played by synaptic pruning not only in developmental plasticity (Huttenlocher 1979; Mataga et al. 2004; Paolicelli et al. 2011), but also in adult cortical plasticity (De Paola et al. 2006; Yamahachi et al. 2009; Keck et al. 2011; van Versendaal et al. 2012; Gilbert and Li 2012).

Conclusions

The coexistence of decreased fast cortical responses and increased slow cortical activations offers a dual perspective of adult cortical plasticity after SCI.

Authors' Contributions

G.F. and J.A. designed the experiments. D.H.V. and J.A. performed all experiments with extracellular and intracellular recordings. E.A.C. and E.F.L. performed all surgical procedures and animal care after spinal cord injury. D.H.V, G.F., and J.A. analyzed the data. D.H.V., J.A., and G.F. wrote the paper.

Funding

This work was supported by Fondo de Investigación Sanitaria del Instituto de Salud Carlos III PI11/02451, co-funded by FEDER, and by Ministerio de Economía y Competitividad SAF2012-40109, co-funded by FEDER.

Notes

We thank to Dr Liset Menéndez-de-la-Prida, Dr Karen Moxon and Dr Casto Rivadulla all criticisms and helpful comments on the manuscript. *Conflict of Interest*: None declared.

References

Aguilar J, Humanes-Valera D, Alonso-Calvino E, Yague JG, Moxon KA, Oliviero A, Foffani G. 2010. Spinal cord injury immediately changes the state of the brain. J Neurosci. 30:7528–7537.

Aguilar J, Pulecchi F, Dilena R, Oliviero A, Priori A, Foffani G. 2011. Spinal direct current stimulation modulates the activity of gracile nucleus and primary somatosensory cortex in anaesthetized rats. J Physiol. 589:4981–4996.

Albieri G, Barnes SJ, de Celis Alonso B, Cheetham CE, Edwards CE, Lowe AS, Karunaratne H, Dear JP, Lee KC, Finnerty GT. 2015. Rapid bidirectional reorganization of cortical microcircuits. Cereb Cortex. 25(9):3025–3035.

Breton JD, Stuart GJ. 2009. Loss of sensory input increases the intrinsic excitability of layer 5 pyramidal neurons in rat barrel cortex. J Physiol. 587:5107–5119.

Buonomano DV, Merzenich MM. 1998. Cortical plasticity: from synapses to maps. Annu Rev Neurosci. 21:149–186.

Butz M, Steenbuck ID, van Ooyen A. 2014. Homeostatic structural plasticity can account for topology changes following deafferentation and focal stroke. Front Neuroanat. 8:115.

Calford MB, Tweedale R. 1988. Immediate and chronic changes in responses of somatosensory cortex in adult flying-fox after digit amputation. Nature. 332:446–448.

Castro-Alamancos MA. 2004a. Absence of rapid sensory adaptation in neocortex during information processing states. Neuron. 41:455–464.

Castro-Alamancos MA. 2009. Cortical up and activated states: implications for sensory information processing. Neuroscientist. 15:625–634.

Castro-Alamancos MA. 2004b. Dynamics of sensory thalamocortical synaptic networks during information processing states. Prog Neurobiol. 74:213–247.

Castro-Alamancos MA, Gulati T. 2014. Neuromodulators produce distinct activated states in neocortex. J Neurosci. 34:12353–12367.

Chapin JK, Lin CS. 1984. Mapping the body representation in the SI cortex of anesthetized and awake rats. J Comp Neurol. 229:199–213.

Cramer SC, Lastra L, Lacourse MG, Cohen MJ. 2005. Brain motor system function after chronic, complete spinal cord injury. Brain. 128:2941–2950.

Curt A, Alkadhi H, Crelier GR, Boendermaker SH, Hepp-Reymond MC, Kollias SS. 2002. Changes of non-affected upper limb cortical representation in paraplegic patients as assessed by fMRI. Brain. 125:2567–2578.

Darian-Smith C, Gilbert CD. 1994. Axonal sprouting accompanies functional reorganization in adult cat striate cortex. Nature. 368:737–740.

Das A, Gilbert CD. 1995. Long-range horizontal connections and their role in cortical reorganization revealed by optical recording of cat primary visual cortex. Nature. 375:780–784.

David F, Schmiedt JT, Taylor HL, Orban G, Di Giovanni G, Uebele VN, Renger JJ, Lambert RC, Leresche N, Crunelli V. 2013. Essential thalamic contribution to slow waves of natural sleep. J Neurosci. 33:19599–19610.

De Paola V, Holtmaat A, Knott G, Song S, Wilbrecht L, Caroni P, Svoboda K. 2006. Cell type-specific structural plasticity of axonal branches and boutons in the adult neocortex. Neuron. 49:861–875.

Endo T, Spenger C, Tominaga T, Brene S, Olson L. 2007. Cortical sensory map rearrangement after spinal cord injury: fMRI responses linked to Nogo signalling. Brain. 130:2951–2961.

Erchova IA, Lebedev MA, Diamond ME. 2002. Somatosensory cortical neuronal population activity across states of anaesthesia. Eur J Neurosci. 15:744–752.

Favero M, Varghese G, Castro-Alamancos MA. 2012. The state of somatosensory cortex during neuromodulation. J Neurophysiol. 108:1010–1024.

Feldmeyer D. 2012. Excitatory neuronal connectivity in the barrel cortex. Front Neuroanat. 6:24.

Flor H, Elbert T, Knecht S, Wienbruch C, Pantev C, Birbaumer N, Larbig W, Taub E. 1995. Phantom-limb pain as a perceptual correlate of cortical reorganization following arm amputation. Nature. 375:482–484.

Florence SL, Taub HB, Kaas JH. 1998. Large-scale sprouting of cortical connections after peripheral injury in adult macaque monkeys. Science. 282:1117–1121.

Foffani G, Humanes-Valera D, Calderon-Munoz F, Oliviero A, Aguilar J. 2011. Spinal cord injury immediately decreases anesthetic requirements in rats. Spinal Cord. 49:822–826.

Foffani G, Shumsky J, Knudsen EB, Ganzer PD, Moxon KA. 2016. Interactive effects between exercise and serotonergic pharmacotherapy on cortical reorganization after spinal cord injury. Neurorehab Neural Repair. 30(5):479–489.

Fouad K, Pedersen V, Schwab ME, Brosamle C. 2001. Cervical sprouting of corticospinal fibers after thoracic spinal cord injury accompanies shifts in evoked motor responses. Curr Biol. 11:1766–1770.

Friedberg MH, Lee SM, Ebner FF. 1999. Modulation of receptive field properties of thalamic somatosensory neurons by the depth of anesthesia. J Neurophysiol. 81:2243–2252.

Gambino F, Pages S, Kehayas V, Baptista D, Tatti R, Carleton A, Holtmaat A. 2014. Sensory-evoked LTP driven by dendritic plateau potentials in vivo. Nature. 515:116–119.

Ganmor E, Katz Y, Lampl I. 2010. Intensity-dependent adaptation of cortical and thalamic neurons is controlled by brainstem circuits of the sensory pathway. Neuron. 66:273–286.

Ganzer PD, Moxon KA, Knudsen EB, Shumsky JS. 2013. Serotonergic pharmacotherapy promotes cortical reorganization after spinal cord injury. Exp Neurol. 241:84–94.

Ganzer PD, Manohar A, Shumsky JS, Moxon KA. 2016. Therapy induces widespread reorganization of motor cortex after complete spinal transection that supports motor recovery. Exp Neurol. 279:1–12.

Ghosh A, Haiss F, Sydekum E, Schneider R, Gullo M, Wyss MT, Mueggler T, Baltes C, Rudin M, Weber B, et al. 2010. Rewiring of hindlimb corticospinal neurons after spinal cord injury. Nat Neurosci. 13:97–104.

Ghosh A, Peduzzi S, Snyder M, Schneider R, Starkey M, Schwab ME. 2012. Heterogeneous spine loss in layer 5 cortical neurons after spinal cord injury. Cereb Cortex. 22:1309–1317.

Giannikopoulos DV, Eysel UT. 2006. Dynamics and specificity of cortical map reorganization after retinal lesions. Proc Natl Acad Sci USA. 103:10805–10810.

Gilbert CD, Li W. 2012. Adult visual cortical plasticity. Neuron. 75:250–264.

Gilbert CD, Wiesel TN. 1992. Receptive field dynamics in adult primary visual cortex. Nature. 356:150–152.

Graziano A, Foffani G, Knudsen EB, Shumsky J, Moxon KA. 2013. Passive exercise of the hind limbs after complete thoracic transection of the spinal cord promotes cortical reorganization. PLoS ONE. 8:e54350.

Grutzendler J, Kasthuri N, Gan WB. 2002. Long-term dendritic spine stability in the adult cortex. Nature. 420:812–816.

Gustin SM, Peck CC, Cheney LB, Macey PM, Murray GM, Henderson LA. 2012. Pain and plasticity: is chronic pain always associated with somatosensory cortex activity and reorganization? J Neurosci. 32:14874–14884.

Harrison TC, Silasi G, Boyd JD, Murphy TH. 2013. Displacement of sensory maps and disorganization of motor cortex after targeted stroke in mice. Stroke. 44:2300–2306.

Hasenstaub A, Sachdev RN, McCormick DA. 2007. State changes rapidly modulate cortical neuronal responsiveness. J Neurosci. 27:9607–9622.

Hirata A, Castro-Alamancos MA. 2010. Neocortex network activation and deactivation states controlled by the thalamus. J Neurophysiol. 103:1147–1157.

Hoffman LR, Field-Fote EC. 2010. Functional and corticomotor changes in individuals with tetraplegia following unimanual or bimanual massed practice training with somatosensory stimulation: a pilot study. J Neurol Phys Therapy. 34:193–201.

Holtmaat AJ, Trachtenberg JT, Wilbrecht L, Shepherd GM, Zhang X, Knott GW, Svoboda K. 2005. Transient and persistent dendritic spines in the neocortex in vivo. Neuron. 45:279–291.

Hubel DH, Wiesel TN, LeVay S. 1977. Plasticity of ocular dominance columns in monkey striate cortex. Philos Trans R Soc Lond Ser B Biol Sci. 278:377–409.

Humanes-Valera D, Aguilar J, Foffani G. 2013. Reorganization of the intact somatosensory cortex immediately after spinal cord injury. PLoS ONE. 8:e69655.

Humanes-Valera D, Foffani G, Aguilar J. 2014. Increased cortical responses to forepaw stimuli immediately after peripheral deafferentation of hindpaw inputs. Sci Rep. 4:7278.

Huttenlocher PR. 1979. Synaptic density in human frontal cortex - developmental changes and effects of aging. Brain Res. 163:195–205.

Jacobs KM, Donoghue JP. 1991. Reshaping the cortical motor map by unmasking latent intracortical connections. Science. 251:944–947.

Jain N, Catania KC, Kaas JH. 1997. Deactivation and reactivation of somatosensory cortex after dorsal spinal cord injury. Nature. 386:495–498.

Jain N, Florence SL, Kaas JH. 1995. Limits on plasticity in somatosensory cortex of adult rats: hindlimb cortex is not reactivated after dorsal column section. J Neurophysiol. 73:1537–1546.

Jones TA, Allred RP, Adkins DL, Hsu JE, O'Bryant A, Maldonado MA. 2009. Remodeling the brain with behavioral experience after stroke. Stroke. 40:S136–S138.

Kaas JH, Krubitzer LA, Chino YM, Langston AL, Polley EH, Blair N. 1990. Reorganization of retinotopic cortical maps in adult mammals after lesions of the retina. Science. 248:229–231.

Kambi N, Halder P, Rajan R, Arora V, Chand P, Arora M, Jain N. 2014. Large-scale reorganization of the somatosensory cortex following spinal cord injuries is due to brainstem plasticity. Nat Commun. 5:3602.

Kao T, Shumsky JS, Murray M, Moxon KA. 2009. Exercise induces cortical plasticity after neonatal spinal cord injury in the rat. J Neurosci. 29:7549–7557.

Katzner S, Nauhaus I, Benucci A, Bonin V, Ringach DL, Carandini M. 2009. Local origin of field potentials in visual cortex. Neuron. 61:35–41.

Keck T, Scheuss V, Jacobsen RI, Wierenga CJ, Eysel UT, Bonhoeffer T, Hubener M. 2011. Loss of sensory input causes rapid structural changes of inhibitory neurons in adult mouse visual cortex. Neuron. 71:869–882.

Kim BG, Dai HN, McAtee M, Bregman BS. 2008. Modulation of dendritic spine remodeling in the motor cortex following spinal cord injury: effects of environmental enrichment and combinatorial treatment with transplants and neurotrophin-3. J Comp Neurol. 508:473–486.

Kim BG, Dai HN, McAtee M, Vicini S, Bregman BS. 2006. Remodeling of synaptic structures in the motor cortex following spinal cord injury. Exp Neurol. 198:401–415.

Levy LM, Ziemann U, Chen R, Cohen LG. 2002. Rapid modulation of GABA in sensorimotor cortex induced by acute deafferentation. Ann Neurol. 52:755–761.

Lilja J, Endo T, Hofstetter C, Westman E, Young J, Olson L, Spenger C. 2006. Blood oxygenation level-dependent visualization of synaptic relay stations of sensory pathways along the neuroaxis in response to graded sensory stimulation of a limb. J Neurosci. 26:6330–6336.

Lotze M, Grodd W, Birbaumer N, Erb M, Huse E, Flor H. 1999. Does use of a myoelectric prosthesis prevent cortical reorganization and phantom limb pain? Nat Neurosci. 2:501–502.

Lotze M, Laubis-Herrmann U, Topka H. 2006. Combination of TMS and fMRI reveals a specific pattern of reorganization in M1 in patients after complete spinal cord injury. Restorative Neurol Neurosci. 24:97–107.

Makin TR, Scholz J, Filippini N, Henderson Slater D, Tracey I, Johansen-Berg H. 2013. Phantom pain is associated with preserved structure and function in the former hand area. Nat Commun. 4:1570.

Manduch M, Bezuhly M, Anastakis DJ, Crawley AP, Mikulis DJ. 2002. Serial fMRI of adaptive changes in primary sensorimotor cortex following thumb reconstruction. Neurology. 59:1278–1281.

Manns ID, Sakmann B, Brecht M. 2004. Sub- and suprathreshold receptive field properties of pyramidal neurones in layers 5A and 5B of rat somatosensory barrel cortex. J Physiol. 556:601–622.

Mataga N, Mizuguchi Y, Hensch TK. 2004. Experience-dependent pruning of dendritic spines in visual cortex by tissue plasminogen activator. Neuron. 44:1031–1041.

Maya Vetencourt JF, Sale A, Viegi A, Baroncelli L, De Pasquale R, O'Leary OF, Castren E, Maffei L. 2008. The antidepressant fluoxetine restores plasticity in the adult visual cortex. Science. 320:385–388.

M'Dahoma S, Bourgoin S, Kayser V, Barthelemy S, Chevarin C, Chali F, Orsal D, Hamon M. 2014. Spinal cord transection-induced allodynia in rats–behavioral, physiopathological and pharmacological characterization. PLoS ONE. 9:e102027.

Megevand P, Troncoso E, Quairiaux C, Muller D, Michel CM, Kiss JZ. 2009. Long-term plasticity in mouse sensorimotor circuits after rhythmic whisker stimulation. J Neurosci. 29:5326–5335.

Mohar B, Katz Y, Lampl I. 2013. Opposite adaptive processing of stimulus intensity in two major nuclei of the somatosensory brainstem. J Neurosci. 33:15394–15400.

Morales-Botello ML, Aguilar J, Foffani G. 2012. Imaging the spatiotemporal dynamics of supragranular activity in the rat

somatosensory cortex in response to stimulation of the paws. PLoS ONE. 7:e40174.
Moxon KA, Hale LL, Aguilar J, Foffani G. 2008. Responses of infragranular neurons in the rat primary somatosensory cortex to forepaw and hindpaw tactile stimuli. Neuroscience. 156:1083–1092.
Moxon KA, Oliviero A, Aguilar J, Foffani G. 2014. Cortical reorganization after spinal cord injury: always for good? Neuroscience. 283:78–94.
Murayama M, Perez-Garci E, Nevian T, Bock T, Senn W, Larkum ME. 2009. Dendritic encoding of sensory stimuli controlled by deep cortical interneurons. Nature. 457:1137–1141.
Murphy TH, Corbett D. 2009. Plasticity during stroke recovery: from synapse to behaviour. Nat Rev Neurosci. 10:861–872.
Nemoto M, Sheth S, Guiou M, Pouratian N, Chen JW, Toga AW. 2004. Functional signal- and paradigm-dependent linear relationships between synaptic activity and hemodynamic responses in rat somatosensory cortex. J Neurosci. 24:3850–3861.
Orlando C, Raineteau O. 2015. Integrity of cortical perineuronal nets influences corticospinal tract plasticity after spinal cord injury. Brain Struct Funct. 220:1077–1091.
Oza CS, Giszter SF. 2014. Plasticity and alterations of trunk motor cortex following spinal cord injury and non-stepping robot and treadmill training. Exp Neurol. 256:57–69.
Oza CS, Giszter SF. 2015. Trunk robot rehabilitation training with active stepping reorganizes and enriches trunk motor cortex representations in spinal transected rats. J Neurosci. 35:7174–7189.
Paolicelli RC, Bolasco G, Pagani F, Maggi L, Scianni M, Panzanelli P, Giustetto M, Ferreira TA, Guiducci E, Dumas L, et al. 2011. Synaptic pruning by microglia is necessary for normal brain development. Science. 333:1456–1458.
Paxinos G, Watson C. 2007. The rat brain in stereotaxic coordinates. Amsterdam: Academic Press.
Petersen CC, Hahn TT, Mehta M, Grinvald A, Sakmann B. 2003. Interaction of sensory responses with spontaneous depolarization in layer 2/3 barrel cortex. Proc Natl Acad Sci USA. 100:13638–13643.
Peyron R, Schneider F, Faillenot I, Convers P, Barral FG, Garcia-Larrea L, Laurent B. 2004. An fMRI study of cortical representation of mechanical allodynia in patients with neuropathic pain. Neurology. 63:1838–1846.
Pizzorusso T, Medini P, Berardi N, Chierzi S, Fawcett JW, Maffei L. 2002. Reactivation of ocular dominance plasticity in the adult visual cortex. Science. 298:1248–1251.
Pons TP, Garraghty PE, Ommaya AK, Kaas JH, Taub E, Mishkin M. 1991. Massive cortical reorganization after sensory deafferentation in adult macaques. Science. 252:1857–1860.
Reig R, Sanchez-Vives MV. 2007. Synaptic transmission and plasticity in an active cortical network. PLoS ONE. 2:e670.
Rigas P, Castro-Alamancos MA. 2007. Thalamocortical up states: differential effects of intrinsic and extrinsic cortical inputs on persistent activity. J Neurosci. 27:4261–4272.
Sachdev RN, Ebner FF, Wilson CJ. 2004. Effect of subthreshold up and down states on the whisker-evoked response in somatosensory cortex. J Neurophysiol. 92:3511–3521.
Sanes JN, Donoghue JP. 2000. Plasticity and primary motor cortex. Annu Rev Neurosci. 23:393–415.
Sanes JN, Suner S, Lando JF, Donoghue JP. 1988. Rapid reorganization of adult rat motor cortex somatic representation patterns after motor nerve injury. Proc Natl Acad Sci USA. 85:2003–2007.
Schmid LM, Rosa MG, Calford MB, Ambler JS. 1996. Visuotopic reorganization in the primary visual cortex of adult cats following monocular and binocular retinal lesions. Cereb Cortex. 6:388–405.
Schnepel P, Kumar A, Zohar M, Aertsen A, Boucsein C. 2015. Physiology and impact of horizontal connections in rat neocortex. Cereb Cortex. 25(10):3818–3835.
Sydekum E, Ghosh A, Gullo M, Baltes C, Schwab M, Rudin M. 2014. Rapid functional reorganization of the forelimb cortical representation after thoracic spinal cord injury in adult rats. NeuroImage. 87:72–79.
van den Brand R, Heutschi J, Barraud Q, DiGiovanna J, Bartholdi K, Huerlimann M, Friedli L, Vollenweider I, Moraud EM, Duis S, et al. 2012. Restoring voluntary control of locomotion after paralyzing spinal cord injury. Science. 336:1182–1185.
van Versendaal D, Rajendran R, Saiepour MH, Klooster J, Smit-Rigter L, Sommeijer JP, De Zeeuw CI, Hofer SB, Heimel JA, Levelt CN. 2012. Elimination of inhibitory synapses is a major component of adult ocular dominance plasticity. Neuron. 74:374–383.
Vessal M, Darian-Smith C. 2010. Adult neurogenesis occurs in primate sensorimotor cortex following cervical dorsal rhizotomy. J Neurosci. 30:8613–8623.
Viaene AN, Petrof I, Sherman SM. 2011a. Synaptic properties of thalamic input to layers 2/3 and 4 of primary somatosensory and auditory cortices. J Neurophysiol. 105:279–292.
Viaene AN, Petrof I, Sherman SM. 2011b. Synaptic properties of thalamic input to the subgranular layers of primary somatosensory and auditory cortices in the mouse. J Neurosci. 31:12738–12747.
Wall PD, Egger MD. 1971. Formation of new connexions in adult rat brains after partial deafferentation. Nature. 232:542–545.
Wester JC, Contreras D. 2012. Columnar interactions determine horizontal propagation of recurrent network activity in neocortex. J Neurosci. 32:5454–5471.
Wiesel TN, Hubel DH. 1963. Effects of visual deprivation on morphology and physiology of cells in the cats lateral geniculate body. J Neurophysiol. 26:978–993.
Wrigley PJ, Gustin SM, Macey PM, Nash PG, Gandevia SC, Macefield VG, Siddall PJ, Henderson LA. 2009a. Anatomical changes in human motor cortex and motor pathways following complete thoracic spinal cord injury. Cereb Cortex. 19:224–232.
Wrigley PJ, Press SR, Gustin SM, Macefield VG, Gandevia SC, Cousins MJ, Middleton JW, Henderson LA, Siddall PJ. 2009b. Neuropathic pain and primary somatosensory cortex reorganization following spinal cord injury. Pain. 141:52–59.
Yague JG, Foffani G, Aguilar J. 2011. Cortical hyperexcitability in response to preserved spinothalamic inputs immediately after spinal cord hemisection. Exp Neurol. 227:252–263.
Yague JG, Humanes-Valera D, Aguilar J, Foffani G. 2014. Functional reorganization of the forepaw cortical representation immediately after thoracic spinal cord hemisection in rats. Exp Neurol. 257:19–24.
Yamahachi H, Marik SA, McManus JN, Denk W, Gilbert CD. 2009. Rapid axonal sprouting and pruning accompany functional reorganization in primary visual cortex. Neuron. 64:719–729.
Zarrinpar A, Callaway EM. 2016. Functional local input to Layer 5 pyramidal neurons in the rat visual cortex. Cereb Cortex. 26(3):991–1003.
Zhang K, Zhang J, Zhou Y, Chen C, Li W, Ma L, Zhang L, Zhao J, Gan W, Zhang L, et al. 2015. Remodeling the dendritic spines in the hindlimb representation of the sensory cortex after spinal cord hemisection in mice. PLoS ONE. 10:e0132077.